

Active Suspension Control With Frequency Band Constraints and Actuator Input Delay

Weichao Sun, Ye Zhao, Jinfu Li, Lixian Zhang, and Huijun Gao, *Senior Member, IEEE*

Abstract—This paper investigates the problem of vehicle active suspension control with frequency band constraints and actuator input delay. First, the mathematical model of suspension systems is established, and the problem of suspension control with finite-frequency constraints is formulated to match the characteristics of the human body. Then, the finite-frequency method is developed to deal with the problem of suspension control with actuator input delay, based on the generalized Kalman–Yakubovich–Popov lemma. Compared with the traditional entire-frequency approach for active suspension systems, the finite-frequency approach proposed in this paper achieves better disturbance attenuation performance for the chosen frequency range while the constraints required by real situation are guaranteed in the controller design. The effectiveness and merits of the proposed method are verified by a number of simulations with several types of road disturbances.

Index Terms—Active suspension systems, actuator input delay, disturbance attenuation, finite frequency.

I. INTRODUCTION

VEHICLE suspensions have been a hot research topic due to their important roles in vehicle performances. Recently, combining active vibration control mechanism with advanced control algorithms to improve suspension systems is a popular and effective way, i.e., the so-called active suspension system which is suitable for improving suspension performances, and has attracted much attention [4], [12], [14], [16], [18], [19], [25].

Generally speaking, performance requirements for vehicle active suspensions include these aspects: ride comfort, which means to isolate passengers from vibration and shock arising from road roughness; handling performance, which refers to suppress the hop of the wheels so as to maintain firm and uninterrupted contact of wheels to road; suspension travel; and actuator consumption. However, these requirements are always conflicting, for example, enhancing ride comfort results in larger suspension stroke and smaller damping in the wheel-

hop mode. Hence, the main goal of active suspension design is to resolve the inherent tradeoffs among ride comfort, handling performance, suspension travel, and actuator consumption. Driven by the aforementioned motivations, a considerable amount of research has been carried out for the last few decades [17], [20], [22], and many active suspension control approaches are proposed, based on various control techniques such as linear quadratic Gaussian control, adaptive control, sliding-mode control [6], [26], nonlinear control, and H_∞ control. In particular, H_∞ control has been intensively discussed in the context of robustness and disturbance attenuation [2], [27], [28].

There are some papers that discuss the problems of H_∞ control or disturbance attenuation for active suspension systems. To mention a few, in [9], the problem of constrained H_∞ control for active suspensions is considered, and a state feedback controller is designed to ensure the disturbance attenuation performance of the closed-loop system while the constraints required in the vehicle suspension control are guaranteed. Finally, the inherent tradeoffs is transformed into the problem of multiobjective control to be addressed. In [7], a load-dependent controller design approach is presented to solve the problem of multiobjective control for vehicle active suspension systems based on the state feedback strategy. This approach of designing controllers, whose gain matrix depends on the online available information of the body mass, is based on a parameter-dependent Lyapunov function, where the performance requirements are fused in the controller design.

As is known to all, time delay is a characteristic that is commonly encountered in various engineering systems, such as pneumatic and hydraulic systems and industrial processes for instance [5], [15]. In active control of vehicle suspension systems, the time delay of the system is an important issue that needs careful treatment to avoid poor performance or even possible instability of the closed-loop system, and unavoidable time delays may appear in the controlled channel, particularly in actuators where the delays are taken to build up the required control force. Although the delay time may be short, it can nevertheless limit the control performance when the delay appears in the feedback loop. There are some results about the active suspension system with actuator input delay, such as [8], [10], and the references therein.

Among the required performances, ride comfort is a key indicator of the active suspension control, and various control strategies have been introduced aiming at improving the ride comfort performance [3], [13]. It is worth mentioning that most researchers design controllers for suspension systems over the entire-frequency range, and the existing results overlook a vital fact that active suspension systems just belong to a certain frequency band. The human body is more sensitive to vibrations of 4–8 Hz in the vertical direction, and human's organs will

Manuscript received June 17, 2010; revised October 14, 2010; accepted February 19, 2011. Date of publication March 28, 2011; date of current version October 4, 2011. This work was supported in part by the 973 Project under Grant 2009CB320600, by the National Natural Science Foundation of China under Grants 60825303 and 61028008, by the Foundation for the Author of National Excellent Doctoral Dissertation of China under Grant 2007B4, by the Fok Ying Tung Education Foundation under Grant 111064, and by the Key Laboratory of Integrated Automation for the Process Industry (Northeastern University), Ministry of Education.

The authors are with the Research Institute of Intelligent Control and Systems, Harbin Institute of Technology, Harbin 150080, China (e-mail: 1984sunweichao@gmail.com; zhaoye8810@gmail.com; ljfking2009@gmail.com; lixianzhanghit@gmail.com; hjgao@hit.edu.cn).

Color versions of one or more of the figures in this paper are available online at <http://ieeexplore.ieee.org>.

Digital Object Identifier 10.1109/TIE.2011.2134057

resonate with the vibrations in this frequency domain. Hence, the development of the finite-frequency control is significative for active suspension systems.

Weighting functions are usually employed in the existing results where the finite-frequency problems are concerned. This weighting method is effective, while it is weighting functions that increase the system complexity, and the process of selecting appropriate weights can be time consuming as well. Recently, a significant development made by Iwasaki and Hara is the generalized Kalman–Yakubovich–Popov (KYP) lemma [23] that establishes the equivalence between a frequency domain property and a linear matrix inequality (LMI) over a finite-frequency range, allowing designers to impose performance requirements over the chosen finite-frequency ranges. The generalized KYP lemma is useful for the analysis and synthesis of practical application problems [1], [11], [24].

In this paper, the problem of vehicle active suspension control with frequency band constraints is considered, where the actuator input delay, limit of actuator output force, and controlled output constraints are taken into account in a unified framework. The quarter-car model is employed as the object of research. By using the generalized KYP lemma, the finite-frequency method is developed to control the active suspension with actuator input delay, and the finite-frequency problems are transformed into a set of LMIs to be solved. In addition, the time-domain constraints, which represent performance requirements for vehicle suspensions (road holding, suspension stroke, and actuator limitation), are guaranteed in the controller design. The desired controllers can be obtained by solving a set of LMIs using standard numerical algorithms. The effectiveness of the proposed approach is shown by an actual example.

The remainder of this paper is organized as follows. The problem of finite-frequency controller design for active suspension systems with input delay is formulated in Section II. Section III presents the results of controller design. The simulations illustrating the usefulness and advantage of the proposed methodology are shown in Section IV, and conclusions are given in Section V. Some essential lemmas are given in the Appendix.

Notation: For a matrix P , P^T , P^{-1} , and P^\perp denote its transpose, inverse, and orthogonal complement, respectively; the notation $P > 0$ (≥ 0) means that P is real symmetric and positive definite (semidefinite); and $[P]_s$ means $P + P^T$. For a vector or matrix, $\{\cdot\}_i$ ($i = 1, 2, \dots$) represents the i th line of the vector or matrix. In symmetric block matrices or complex matrix expressions, we use an asterisk ($*$) to represent a term that is induced by symmetry, and $\text{diag}\{\dots\}$ stands for a block-diagonal matrix. Matrices, if their dimensions are not explicitly stated, are assumed to be compatible for algebraic operations. The space of square-integrable vector functions over $[0, \infty)$ is denoted by $L_2[0, \infty)$, and for $w = \{w(t)\} \in L_2[0, \infty)$, its norm is given by $\|w\|_2 = \sqrt{\int_{t=0}^{\infty} |w(t)|^2 dt}$. For $G \in \mathbb{C}^{n \times m}$ and $\Pi \in \mathbf{H}_{n+m}$, a function $v: \mathbb{C}^{n \times m} \times \mathbf{H}_{n+m} \rightarrow \mathbf{H}_m$ is defined by $v(G, \Pi) = \begin{bmatrix} G \\ I_m \end{bmatrix}^* \Pi \begin{bmatrix} G \\ I_m \end{bmatrix}$.

II. PROBLEM FORMULATION

By considering the vertical dynamics and taking into account the vehicle's symmetry, a suspension can be reduced to a

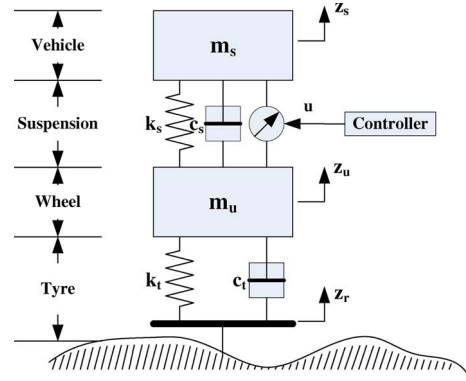


Fig. 1. Quarter-car model with an active suspension.

quarter-car model, as shown in Fig. 1. In this figure, m_s is the sprung mass, m_u is the unsprung mass; c_s and k_s are the damping and stiffness of the suspension system, respectively; k_t and c_t stand for compressibility and damping of the pneumatic tire, respectively; z_s and z_u are the displacements of the sprung and unsprung masses, respectively; z_r is the road displacement input; and u is the active input of the suspension system. In this paper, the effect of actuator dynamics is neglected, and the actuator is modeled as an ideal force generator.

The ideal dynamic equations of the sprung and unsprung masses are given in [8]. Define the following state variables:

$$\begin{aligned} x_1(t) &= z_s(t) - z_u(t) & x_2(t) &= z_u(t) - z_r(t) \\ x_3(t) &= \dot{z}_s(t) & x_4(t) &= \dot{z}_u(t) \end{aligned} \quad (1)$$

and the disturbance input is defined as $w(t) = \dot{z}_r(t)$.

Then, by defining

$$x(t) = [x_1(t) \quad x_2(t) \quad x_3(t) \quad x_4(t)]^T$$

we have the following state-space form:

$$\dot{x}(t) = Ax(t) + B_1w(t) + Bu(t) \quad (2)$$

where

$$A = \begin{bmatrix} 0 & 0 & 1 & -1 \\ 0 & 0 & 0 & 1 \\ -\frac{k_s}{m_s} & 0 & -\frac{c_s}{m_s} & \frac{c_s}{m_s} \\ \frac{k_s}{m_u} & -\frac{k_u}{m_u} & \frac{c_s}{m_u} & -\frac{c_s+c_t}{m_u} \end{bmatrix} \quad (3)$$

$$B = \begin{bmatrix} 0 & 0 & \frac{1}{m_s} & -\frac{1}{m_u} \end{bmatrix}^T \quad (3)$$

$$B_1 = \begin{bmatrix} 0 & -1 & 0 & \frac{c_t}{m_u} \end{bmatrix}^T. \quad (4)$$

A. Ride Comfort

It is widely accepted that ride comfort is closely related to the body acceleration in the 4–8-Hz frequency band. Consequently, it is important to keep the L_2 gain (from the disturbance inputs to car body acceleration) of the closed-loop system as small as possible over the 4–8-Hz frequency band.

B. Road Holding Ability

Due to the disturbances caused by road bumpiness, a firm uninterrupted contact of wheels with the road is important for vehicle handling and is essentially related to ride safety.

Therefore, the dynamic tire load should be small, i.e., $k_t(z_u(t) - z_r(t)) < (m_s + m_u)g$.

C. Suspension Deflection

To reduce the vertical acceleration of the car body, it is unavoidable to use more suspension travel, which increases the likelihood of a driver hitting the suspension travel limits when driving over a speed bump or into a pothole. Hence, the suspension deflection should travel within its allowable range, i.e., $|z_s(t) - z_u(t)| \leq z_{\max}$, where z_{\max} is the maximum suspension deflection.

D. Actuator Limitation

As the operator of a control system, the actuator plays an important role in engineering applications [21]. Here, another hard constraint imposed on active suspensions is from the limited power of the actuator, i.e., $|u(t)| \leq u_{\max}$.

In order to satisfy the aforementioned performance requirements, the controlled outputs are defined by

$$\begin{aligned} z_1(t) &= \ddot{z}_s(t), \\ z_2(t) &= \begin{bmatrix} \frac{z_s(t) - z_u(t)}{z_{\max}} & \frac{k_t(z_u(t) - z_r(t))}{(m_s + m_u)g} \end{bmatrix}^T. \end{aligned} \quad (5)$$

Therefore, the vehicle suspension control system can be described by

$$\begin{aligned} \dot{x}(t) &= Ax(t) + Bu(t) + B_1w(t) \\ z_1(t) &= C_1x(t) + D_1u(t) \\ z_2(t) &= C_2x(t) \end{aligned} \quad (6)$$

where

$$\begin{aligned} C_1 &= \begin{bmatrix} -\frac{k_s}{m_s} & 0 & -\frac{c_s}{m_s} & \frac{c_s}{m_s} \end{bmatrix} & D_1 &= \frac{1}{m_s} \\ C_2 &= \begin{bmatrix} \frac{1}{z_{\max}} & 0 & 0 & 0 \\ 0 & \frac{k_t}{(m_s + m_u)g} & 0 & 0 \end{bmatrix}. \end{aligned}$$

Time delays are widely encountered in the control loops because of the electrical and electromagnetic characteristics of the actuators. In this paper, the results of finite-frequency control are developed to address the active suspension systems with input time delay.

We are interested in designing a state feedback controller

$$u(t) = Kx(t) \quad (7)$$

where K is the state feedback gain matrix to be designed. Therefore, the closed-loop system is given by

$$\begin{aligned} \dot{x}(t) &= Ax(t) + BKx(t-d) + B_1w(t) \\ z_1(t) &= C_1x(t) + D_1Kx(t-d) \\ z_2(t) &= C_2x(t). \end{aligned} \quad (8)$$

In this paper, our purpose is to design a state feedback gain matrix K such that the following conditions are satisfied.

- 1) The closed-loop system in (8) is asymptotically stable.
- 2) The L_2 gain of the closed-loop system should be smaller or less than a certain given value γ within the chosen frequency band, i.e.,

$$\|z_1(j\omega)\|_2 < \gamma \|w(j\omega)\|_2, \quad \omega_1 < \omega < \omega_2. \quad (9)$$

- 3) The following constraints are guaranteed with the disturbance energy under the bound w_{\max} :

$$\begin{aligned} |\{z_2(t)\}_i| &\leq 1, \quad i = 1, 2 \\ |u(t)| &\leq u_{\max}. \end{aligned} \quad (10)$$

III. FINITE-FREQUENCY CONTROLLER DESIGN

In this section, the finite-frequency controller will be designed to address the active suspension systems with actuator input delay, and the following theorem gives the conclusion of controller design.

Theorem 1: Give positive scalars γ , α , β_1 , β_2 , and ρ , and let a state feedback controller in the form of (7) be given. The closed-loop system in (8) is asymptotically stable and satisfies $\|z_1(j\omega)\|_2 < \gamma \|w(j\omega)\|_2$, for $\omega \in [\omega_1, \omega_2]$, while respecting the constraints in (10) with the disturbance energy under the bound $w_{\max} = (\rho - V'(0))/\eta$, if there exist symmetric matrices P , $S_1 > 0$, $S_2 > 0$, $R_1 > 0$, $R_2 > 0$, $P_1 > 0$, $P_2 > 0$, and $Q > 0$ and general matrices K and Y satisfying

$$\Pi_1 + [Y_1U_1]_s < 0 \quad (11)$$

$$\Theta + M + [Y_2U_2]_s < 0 \quad (12)$$

$$\begin{bmatrix} -I & \sqrt{\rho}\{C_2\}_i \\ * & -P_2 \end{bmatrix} < 0 \quad (13)$$

$$\begin{bmatrix} -I & \sqrt{\rho}K \\ * & -u_{\max}^2P_2 \end{bmatrix} < 0 \quad (14)$$

where

$$\begin{aligned} \Pi_1 &= \begin{bmatrix} d^2S_1 & P_1 & 0 \\ * & R_1 - S_1 & S_1 \\ * & * & -R_1 - S_1 \end{bmatrix} \\ \Pi_2 &= \begin{bmatrix} d^2S_2 & P_2 & 0 \\ * & R_2 - S_2 & S_2 \\ * & * & -R_2 - S_2 \end{bmatrix} \\ Y_1 &= [Y^T \quad \alpha Y^T \quad 0]^T \\ Y_2 &= [\beta_1 Y^T \quad \beta_2 Y^T \quad 0 \quad 0]^T \\ U_1 &= [-I \quad A \quad BK] \\ U_2 &= [-I \quad A \quad BK \quad B_1] \\ L &= [0 \quad C_1 \quad D_1K] \\ \Theta &= \begin{bmatrix} \Pi_2 + L^T L & 0 \\ * & -\gamma^2 I \end{bmatrix} \\ F &= \begin{bmatrix} I & 0 & 0 & 0 \\ 0 & I & 0 & 0 \end{bmatrix} & \Phi &= \begin{bmatrix} 0 & 1 \\ 1 & 0 \end{bmatrix} \\ M &= F^*(\Phi \otimes P + \Psi \otimes Q)F \\ \Psi &= \begin{bmatrix} -1 & j\omega_c \\ -j\omega_c & -\omega_1\omega_2 \end{bmatrix}. \end{aligned}$$

Proof: First, the asymptotic stability of (8) with $w(t) = 0$ is shown, i.e.,

$$\dot{x}(t) = Ax(t) + BKx(t-d). \quad (15)$$

Consider a Lyapunov functional candidate as

$$V(t) \triangleq V_1(t) + V_2(t) + V_3(t) \quad (16)$$

$$V_1(t) \triangleq x^T(t)P_1x(t) \quad (17)$$

$$V_2(t) \triangleq \int_{t-d}^t x^T(s)R_1x(s) ds \quad (18)$$

$$V_3(t) \triangleq d \int_{-d}^0 \int_{t+\beta}^t \dot{x}^T(\alpha)S_1\dot{x}(\alpha) d\alpha d\beta \quad (19)$$

where $P_1 > 0$, $R_1 > 0$, and $S_1 > 0$ are matrices to be determined.

The derivatives of $V_1(t)$, $V_2(t)$, and $V_3(t)$ satisfy

$$\begin{aligned} \dot{V}_1(t) &= \dot{x}^T(t)P_1x(t) + x^T(t)P_1\dot{x}(t) \\ \dot{V}_2(t) &= x^T(t)R_1x(t) - x^T(t-d)R_1x(t-d) \\ \dot{V}_3(t) &= d^2\dot{x}^T(t)S_1\dot{x}(t) - d \int_{t-d}^t \dot{x}^T(\beta)S_1\dot{x}(\beta) d\beta. \end{aligned}$$

By using the Jensen inequality in Lemma 1, we have

$$\begin{aligned} -d \int_{t-d}^t \dot{x}^T(\beta)S_1\dot{x}(\beta) d\beta \\ \leq -[x(t) - x(t-d)]^T S_1 [x(t) - x(t-d)]. \end{aligned}$$

Then, we have $\dot{V}(t) \leq \zeta^T(t)\Pi_1\zeta(t)$, where $\zeta(t) = [\dot{x}^T(t) \ x^T(t) \ x^T(t-d)]^T$. On the other hand, from Lemma 2, inequality (11) is equivalent to

$$\delta^T(t)\Pi_1\delta(t) < 0 \quad \forall U_1\delta(t) = 0$$

which can guarantee $\dot{V}(t) < 0$ from the fact that $U_1\zeta(t) = 0$, which means that the closed-loop system in (8) is asymptotically stable.

Next, we shall establish the L_2 gain performance of the closed-loop system in (9). Choose a Lyapunov functional as

$$V'(t) \triangleq V_1'(t) + V_2'(t) + V_3'(t) \quad (20)$$

$$V_1'(t) \triangleq x^T(t)P_2x(t) \quad (21)$$

$$V_2'(t) \triangleq \int_{t-d}^t x^T(s)R_2x(s) ds \quad (22)$$

$$V_3'(t) \triangleq \int_{-d}^0 \int_{t+\beta}^t \dot{x}^T(\alpha)S_2\dot{x}(\alpha) d\alpha d\beta \quad (23)$$

where $P_2 > 0$, $R_2 > 0$, and $S_2 > 0$ are matrices to be determined. Then, we can obtain

$$\dot{V}'(t) \leq \zeta^T(t)\Pi_2\zeta(t). \quad (24)$$

Define

$$J \triangleq \|z_1\|_2^2 - \gamma^2\|w\|_2^2. \quad (25)$$

Under zero initial conditions, we can obtain

$$\begin{aligned} J &\leq \|z_1\|_2^2 - \gamma^2\|w\|_2^2 + V'(\infty) - V'(0) \\ &= \int_0^\infty \left(z_1^T z_1 - \gamma^2 w^T w + \dot{V}'(t) \right) dt \end{aligned} \quad (26)$$

$$\leq \int_0^\infty \xi^T(t)\Theta\xi(t) dt \quad (27)$$

where $\xi(t) \triangleq [\zeta^T(t) \ w^T(t)]^T$. Define

$$\bar{J} = \int_0^\infty \xi^T(t)\Theta\xi(t) dt. \quad (28)$$

Noting that Θ is a real symmetric matrix, we can split Θ as $\Theta = (\Theta^{1/2})^* \Theta^{1/2}$, and we can get

$$\bar{J} = \int_0^\infty \phi^*(t)\phi(t) dt, \quad \text{with } \phi(t) = \Theta^{\frac{1}{2}}\xi(t). \quad (29)$$

After the Fourier transform to $\phi(t)$, we can obtain the spectrum of $\phi(t)$, which is denoted as $\phi_s(\omega)$. By using the Parseval equality, we have

$$\begin{aligned} \bar{J} &= \int_0^\infty \phi^*(t)\phi(t) dt = \frac{1}{2\pi} \int_{-\infty}^\infty \phi_s^*(\omega)\phi_s(\omega) d\omega \\ &= \frac{1}{2\pi} \int_{-\infty}^\infty \xi_s^*(\omega)\Theta\xi_s(\omega) d\omega. \end{aligned} \quad (30)$$

On the other hand, Lemma 2 tells us that inequality (12) is equivalent to

$$\begin{aligned} \xi_s^*(\omega)(\Theta + M)\xi_s(\omega) &< 0 \\ U_2\xi_s(\omega) &= 0 \end{aligned} \quad (31)$$

where inequality (31) can guarantee

$$\xi_s^*(\omega)\Theta\xi_s(\omega) < 0 \quad \text{with } \xi_s^*(\omega)M\xi_s(\omega) \geq 0 \quad (32)$$

by using the S -procedure.

Define

$$\mathbf{M} = \{F^*(\Phi \otimes P + \Psi \otimes Q)F; P, Q \in \mathbf{H}_2\}$$

$$\mathbf{E} = \{s = \mathbb{C} : v(s, \Phi) = 0, v(s, \Psi) \geq 0\}.$$

From [23], we know that the following two sets are equivalent:

$$\mathbf{W}_{(1)} = \{\varepsilon \in \mathbb{C} : \varepsilon \neq 0, \varepsilon^* M \varepsilon \geq 0, \exists M \in \mathbf{M}\}$$

$$\mathbf{W}_{(2)} = \{\varepsilon \in \mathbb{C} : \varepsilon \neq 0, T_s F \varepsilon = 0, s \in \mathbf{E}\}$$

and $\mathbf{W}_{(2)}$ describes our chosen frequency band $\omega \in [\omega_1, \omega_2]$, with

$$\Phi = \begin{bmatrix} 0 & 1 \\ 1 & 0 \end{bmatrix} \quad \Psi = \begin{bmatrix} -1 & j\omega_c \\ -j\omega_c & -\omega_1\omega_2 \end{bmatrix}.$$

Therefore, we can see that inequality (32) guarantees $J < 0$, which implies that $\|z_1(j\omega)\|_2 < \gamma\|w(j\omega)\|_2$ with $\omega \in [\omega_1, \omega_2]$. Inequality (9) is guaranteed.

From the aforementioned proof, we can see that inequality (32) can guarantee $\bar{J} < 0$, which implies that

$$z_1^T z_1 - \gamma^2 w^T w + \dot{V}'_1(t) < 0 \quad (33)$$

and then, inequality (33) guarantees that

$$\dot{V}'_1(t) < \gamma^2 w^T w. \quad (34)$$

Integrating both sides of inequality (34) from 0 to t results in

$$V'(t) - V'(0) < \gamma^2 \int_0^t w^T(t)w(t) dt \leq \gamma^2 w_{\max}$$

where $w_{\max} = \|w\|_2^2$. Note that $V_2'(t) > 0$, $V_3'(t) > 0$, which shows that

$$x^T(t)P_2x(t) < V'(0) + \gamma^2 w_{\max} = \rho. \quad (35)$$

Consider

$$\begin{aligned} \max_{t \geq 0} \{|z_2(t)\}_i|^2 &= \max_{t \geq 0} (x^T(t)\{C_2\}_i^T\{C_2\}_i x(t)) \\ \max_{t \geq 0} |u(t)|^2 &= \max_{t \geq 0} (x^T(t)K^T K x(t)). \end{aligned}$$

From inequality (35), it is true that

$$\begin{aligned} \max_{t \geq 0} \{|z_2(t)\}_i|^2 &< \rho \cdot \lambda_{\max} \left(P_2^{-\frac{1}{2}} \{C_2\}_i^T \{C_2\}_i P_2^{-\frac{1}{2}} \right) \\ \max_{t \geq 0} |u(t)|^2 &< \rho \cdot \lambda_{\max} \left(P_2^{-\frac{1}{2}} K^T K P_2^{-\frac{1}{2}} \right) \end{aligned}$$

where $\lambda_{\max}(\cdot)$ represents the maximum eigenvalue. Then, the constraints in (10) hold if

$$\begin{aligned} \rho P_2^{-\frac{1}{2}} \{C_2\}_i^T \{C_2\}_i P_2^{-\frac{1}{2}} &< I, \quad i = 1, 2 \\ \rho P_2^{-\frac{1}{2}} K^T K P_2^{-\frac{1}{2}} &< u_{\max}^2 I \end{aligned} \quad (36)$$

which, by Schur complement, are equivalent to (14). The proof is completed. ■

Define $\hat{J}_1 = \text{diag}\{Y^{-1}, Y^{-1}, Y^{-1}\}$, $\hat{J}_2 = \text{diag}\{Y^{-1}, Y^{-1}, Y^{-1}, I, I\}$, $\hat{J}_3 = \text{diag}\{I, Y^{-1}\}$, and $\hat{J}_4 = \text{diag}\{I, Y^{-1}\}$. Then, we perform a congruence transformation to (11)–(14), respectively, by the full rank matrices \hat{J}_1 , \hat{J}_2 , \hat{J}_3 , and \hat{J}_4 on the left and \hat{J}_1^T , \hat{J}_2^T , \hat{J}_3^T , and \hat{J}_4^T on the right. Defining

$$\begin{aligned} \bar{S}_1 &= Y^{-1} S_1 Y^{-T} & \bar{P}_1 &= Y^{-1} P_1 Y^{-T} & \bar{Y} &= Y^{-1} \\ \bar{R}_1 &= Y^{-1} R_1 Y^{-T} & \bar{R}_2 &= Y^{-1} R_1 Y^{-T} & \bar{K} &= K Y^{-T} \\ \bar{S}_2 &= Y^{-1} S_1 Y^{-T} & \bar{P}_2 &= Y^{-1} P_1 Y^{-T} \end{aligned}$$

we have the following solvable theorem.

Theorem 2: Give positive scalars γ , α , β_1 , β_2 , and ρ , and let a state feedback controller in the form of (7) be given. The closed-loop system in (8) is asymptotically stable and satisfies $\|z_1(j\omega)\|_2 < \gamma \|w(j\omega)\|_2$, for $\omega \in [\omega_1, \omega_2]$, while respecting the constraints in (10) with the disturbance energy under the bound $w_{\max} = (\rho - V'(0))/\eta$, if there exist symmetric matrices \bar{P} , $\bar{S}_1 > 0$, $\bar{S}_2 > 0$, $\bar{P}_1 > 0$, $\bar{P}_2 > 0$, $\bar{R}_1 > 0$, $\bar{R}_2 > 0$, and $\bar{Q} > 0$ and general matrices \bar{Y} , \bar{K} , satisfying inequality (37)–(40), shown at bottom of the next page.

Moreover, the control gain K is given by $K = \bar{K}\bar{Y}^{-T}$.

IV. SIMULATION

In this section, we will apply the aforementioned approach to design a state feedback controller based on the quarter-car model described in Section II. The quarter-car model parameters are shown as $m_s = 320$ kg, $m_u = 40$ kg, $k_s = 18$ kN/m, $k_t = 200$ kN/m, $c_s = 1$ kN · s/m, and $c_t = 10$ N · s/m.

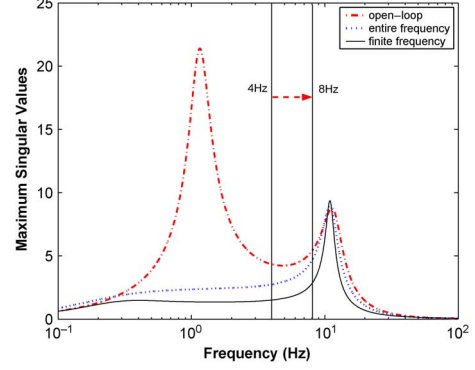


Fig. 2. Curves of MSVs ($d = 5$ ms).

By solving the matrix inequalities (37)–(40) with $\omega_1 = 4$ Hz, $\omega_2 = 8$ Hz, $\rho = 0.01$, and $z_{\max} = 100$ mm and choosing $d = 5$ ms, we can obtain $\gamma_{\min} = 8.4059$, and

$$K = 10^4 \times [1.6985 \quad 0.5127 \quad 0.0180 \quad -0.0654].$$

Then, we will solve the entire-frequency controller, according in [8]. After solving the matrix inequalities in [8] with $d = 5$ ms, we can calculate $\gamma_{\min} = 16.1799$, and

$$K = 10^4 \times [1.7799 \quad 0.2873 \quad 0.0485 \quad -0.0308].$$

After obtaining the finite- and entire-frequency controllers, we will compare the two controllers to illustrate the performance of the closed-loop suspension system with actuator time delay in the finite-frequency domain. In Fig. 2, the solid and dotted lines are the responses of the closed-loop system with the finite- and entire-frequency controllers, respectively, and the dashed line is the response of the passive system. From the figure, we can see that the finite-frequency controller yields the least maximum singular values (MSVs) over the frequency range 4–8 Hz, for the active suspension systems with input delay ($d = 5$ ms), which clearly shows that an improved ride comfort has been achieved.

In order to evaluate the suspension characteristics with respect to the performance requirements, we give the disturbance signal in (41) to clarify the effectiveness of our finite-frequency controller

$$w(t) = \begin{cases} A \sin(2\pi ft), & \text{if } 0 \leq t \leq T \\ 0, & \text{if } t > T. \end{cases} \quad (41)$$

Assume that $A = 0.5$ m, $f = 5$ Hz, and $T = 1/f = 0.2$ s, and the time-domain response of body vertical acceleration for the active suspension system is shown in Fig. 3, where the black solid line and the blue dashed line are the responses of body vertical acceleration with the finite- and entire-frequency controllers, respectively. We can clearly see that the value of the body acceleration with the finite-frequency controller is less than that with the entire-frequency controller. In addition, Fig. 4 shows that the ratio $x_1(t)/z_{\max}$ and the relative dynamic tire load $k_t x_2(t)/(m_s + m_u)g$ are below one, which means that the time-domain constraints are guaranteed by the designed controller. Also, the force of actuator is below the maximum 2500 N.

When the actuator time delay is increased to 20 ms, the MSVs of the passive suspension, the active suspension with entire-frequency controller, and the active suspension with

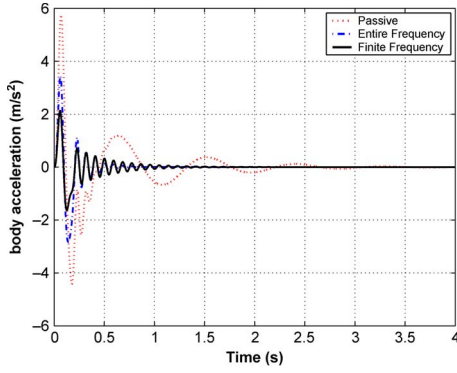


Fig. 3. Time-domain response of body acceleration ($d = 5$ ms).

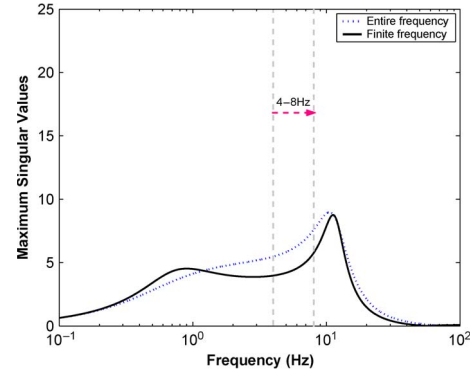


Fig. 5. Curves of MSVs with ($d = 20$ ms).

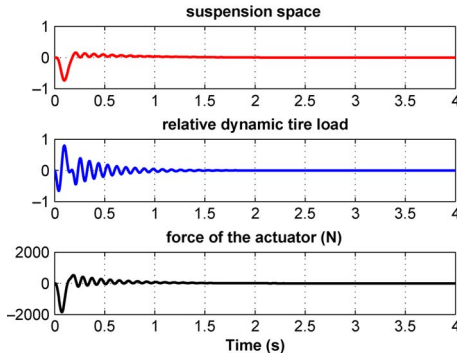


Fig. 4. Constraints of suspension system ($d = 5$ ms).

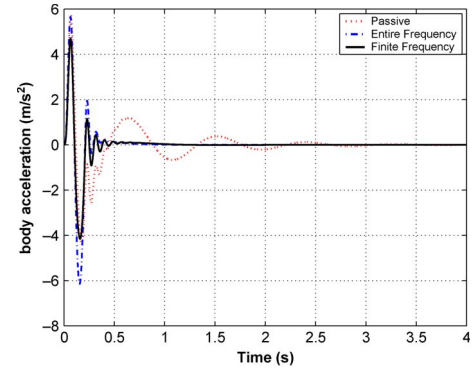


Fig. 6. Time-domain response of body acceleration ($d = 20$ ms).

finite-frequency controller are compared in Fig. 5, which shows the same conclusion with the case $d = 5$ ms. However, as the actuator delay increases, disturbance attenuation becomes weaker than the case of $d = 5$ ms, which also implies the impact of actuator time delay on the suspension system.

The time-domain responses of the body acceleration, suspension deflection limitation, relative tire dynamic load, and active force are shown in Figs. 6 and 7. It can be seen from these figures that the responses of the body acceleration, the suspension deflection limitation, the relative tire dynamic load, and the active force of active suspension are all similar to those shown in Figs. 3 and 4 in spite of the increase of time delay.

Hereinafter, another disturbance signal is used to verify the effectiveness of the designed controller, i.e., the random vibration. Random vibrations are consistent and typically specified as a random process with a given ground displacement power spectral density (PSD) of

$$G_q(n) = G_q(n_0) \left(\frac{n}{n_0} \right)^{-W} \quad (42)$$

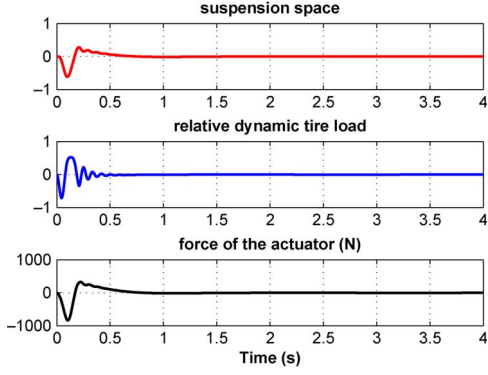
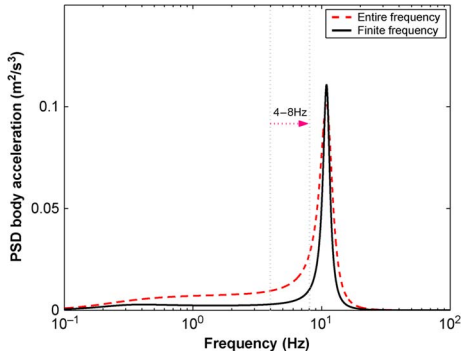
where n is the spatial frequency, n_0 is the reference spatial frequency of $n_0 = 0.1(1/m)$, $G_q(n_0)$ stands for the road roughness coefficient, and $W = 2$ is the road roughness constant.

$$\begin{bmatrix} d^2 \bar{S}_1 - [\bar{Y}]_s & \bar{P}_1 + A\bar{Y}^T - \alpha\bar{Y} & B\bar{K} \\ * & \bar{R}_1 - \bar{S}_1 + [\alpha A\bar{Y}^T]_s & \bar{S}_1 + \alpha B\bar{K} \\ * & * & -\bar{R}_1 - \bar{S}_1 \end{bmatrix} > 0 \quad (37)$$

$$\begin{bmatrix} \left(\begin{array}{c} d^2 \bar{S}_2 - \bar{Q} \\ -\beta_1 [\bar{Y}]_s \end{array} \right) & \left(\begin{array}{c} \bar{P}_2 + \bar{P} + j\omega_c \bar{Q} \\ +\beta_1 A\bar{Y}^T - \beta_2 \bar{Y} \end{array} \right) & \beta_1 B\bar{K} & \beta_1 B_1 & 0 \\ * & \left(\begin{array}{c} \bar{R}_2 - \bar{S}_2 - \omega_1 \omega_2 \bar{Q} \\ +\beta_2 [A\bar{Y}^T]_s \end{array} \right) & \beta_2 B\bar{K} + \bar{S}_2 & \beta_2 B_1 & \bar{Y}C^T \\ * & * & -\bar{R}_2 - \bar{S}_2 & 0 & \bar{K}^T D_1^T \\ * & * & * & -\gamma^2 I & 0 \\ * & * & * & * & -I \end{bmatrix} > 0 \quad (38)$$

$$\begin{bmatrix} -I & \sqrt{\rho} \{C_2\}_i \bar{Y}^T \\ * & -\bar{P}_2 \end{bmatrix} > 0 \quad (39)$$

$$\begin{bmatrix} -I & \sqrt{\rho} \bar{K} \\ * & -u_{\max}^2 \bar{P}_2 \end{bmatrix} > 0 \quad (40)$$

Fig. 7. Constraints of suspension system ($d = 20$ ms).Fig. 8. PSD of body acceleration ($d = 5$ ms).

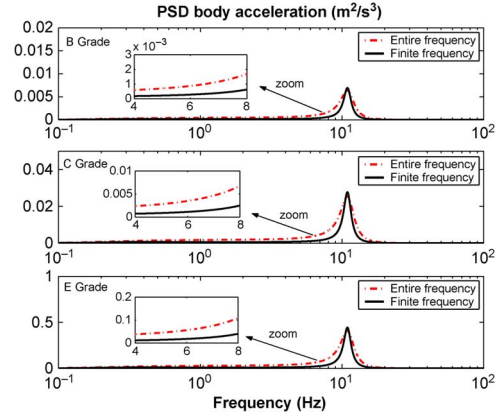
Related to the time frequency f , we have $f = nV$ with V for the vehicle forward velocity. According to (42), we can obtain the PSD ground displacement as $G_q(f) = G_q(n_0)n_0^2(V/f^2)$. Correspondingly, PSD ground velocity is given by

$$G_{\dot{q}}(f) = (2\pi f)^2 G_q(f) = 4\pi G_q(n_0)n_0^2 V \quad (43)$$

which is only related with the vehicle forward velocity. Select the road roughness as $G_q(n_0) = 256 \times 10^{-6} \text{ m}^3$, which corresponds to D grade (poor) according to ISO2361 standards, to generate the random road profile. Set the vehicle forward velocity as $V = 45 \text{ km/h}$, and as expected, it is observed from Fig. 8 that the closed-loop system with finite-frequency controller realizes a better ride comfort compared with the system with entire-frequency controller for the frequency range 4–8 Hz (since the closed-loop system with finite-frequency controller has lower PSD body acceleration than that with entire-frequency controller and smaller PSD body acceleration value results in better ride comfort), where PSD body acceleration can be calculated by

$$G_{z_1}(f) = |G(j\omega)|^2 G_{\dot{q}}(f). \quad (44)$$

To check more random road profiles, we select the road roughness as $G_q(n_0) = 16 \times 10^{-6} \text{ m}^3$ (B grade—good), $G_q(n_0) = 64 \times 10^{-6} \text{ m}^3$ (C grade—average), and $G_q(n_0) = 1024 \times 10^{-6} \text{ m}^3$ (E grade—very poor), respectively. From Fig. 9, it can be observed that the closed-loop system with finite-frequency controller realizes a better ride comfort than that with the traditional method in spite of the different road roughness. When the actuator time delay is not 5 ms but the

Fig. 9. PSD of body acceleration with different road profiles ($d = 5$ ms).

other value, the control results are with the similar situation, and here, we pass the repetition over.

V. CONCLUDING REMARKS

In this paper, the finite-frequency method has been developed to deal with the active suspension systems with actuator input delay, and the state feedback controller for active suspension systems with frequency band constraints has been designed to improve ride comfort. The key idea of designing the proposed controllers is to use the generalized KYP lemma. At the same time, the time-domain constraints have also been guaranteed in the controller design. Simulation results show that the finite-frequency controllers achieve better disturbance attenuation performance over the concerned frequency range than those designed in the entire frequency.

APPENDIX

Lemma 1—(Jensen Inequality): For any positive symmetric constant matrix $M \in R^{n \times n}$, scalar r satisfying $r > 0$, and a vector function $\omega : [0, r] \rightarrow R_n$ such that the integrations concerned are well defined, then

$$r \int_0^r \omega^T(s) M \omega(s) ds \geq \left(\int_0^r \omega(s) ds \right)^T M \int_0^r \omega(s) ds.$$

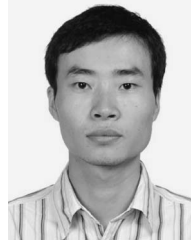
Lemma 2—(Finsler's Lemma): Let $x \in R_n$, $P \in S_n$, and $H \in R^{m \times n}$ such that $\text{rank}(H) = r < n$. The following statements are equivalent:

$$\begin{aligned} x^T P x < 0 \quad \forall Hx = 0, \quad x \neq 0 \\ \Leftrightarrow \exists X \in R^{n \times m} : P + XH + H^T X^T < 0. \end{aligned}$$

REFERENCES

- [1] B. Hency and A. Alleyne, "A KYP lemma for LMI regions," *IEEE Trans. Autom. Control*, vol. 52, no. 10, pp. 1926–1930, Oct. 2007.
- [2] B. Shen, Z. Wang, H. Shu, and G. Wei, "On nonlinear H_∞ filtering for discrete-time stochastic systems with missing measurements," *IEEE Trans. Autom. Control*, vol. 53, no. 9, pp. 2170–2180, Oct. 2008.
- [3] C. Kaddissi, J. P. Kenné, and M. Saad, "Drive by wire control of an electro-hydraulic active suspension a backstepping approach," in *Proc. IEEE Conf. Control Appl.*, Toronto, ON, Canada, Aug. 28–31, 2005, pp. 1581–1587.

- [4] C. García-Rodríguez, J. Cortés-Romero, and H. Sira-Ramírez, "Algebraic identification and discontinuous control for trajectory tracking in a perturbed 1-DOF suspension system," *IEEE Trans. Ind. Electron.*, vol. 56, no. 9, pp. 3665–3674, Sep. 2009.
- [5] E. Boukas and N. M'Sirdi, "Stabilization of linear systems via delayed state feedback controller," *ICIC Exp. Lett.*, vol. 2, no. 1, pp. 1–6, 2008.
- [6] E. Kayacan, Y. Oniz, and O. Kaynak, "A grey system modeling approach for sliding-mode control of antilock braking system," *IEEE Trans. Ind. Electron.*, vol. 56, no. 8, pp. 3244–3252, Aug. 2009.
- [7] H. Gao, J. Lam, and C. Wang, "Multi-objective control of vehicle active suspension systems via load-dependent controllers," *J. Sound Vib.*, vol. 290, no. 3–5, pp. 645–675, Mar. 2006.
- [8] H. Gao, W. Sun, and P. Shi, "Robust sampled-data H_∞ control for vehicle active suspension systems," *IEEE Trans. Control Syst. Technol.*, vol. 18, no. 1, pp. 238–245, Jan. 2010.
- [9] H. Chen and K. Guo, "Constrained H_∞ control of active suspensions: An LMI approach," *IEEE Trans. Control Syst. Technol.*, vol. 13, no. 3, pp. 412–421, May 2005.
- [10] H. Du and N. Zhang, " H_∞ control of active vehicle suspensions with actuator time delay," *J. Sound Vib.*, vol. 301, no. 1/2, pp. 236–252, Mar. 2007.
- [11] H. Khatibi, A. Karimi, and R. Longchamp, "Fixed-order controller design for polytopic systems using LMIs," *IEEE Trans. Autom. Control*, vol. 53, no. 1, pp. 428–434, Feb. 2008.
- [12] H. Kim, H. Yang, and Y. Park, "Improving the vehicle performance with active suspension using road-sensing algorithm," *Comput. Struct.*, vol. 80, no. 18/19, pp. 1569–1577, Jul. 2002.
- [13] I. Fialho and G. J. Balas, "Road adaptive active suspension design using linear parameter-varying gain-scheduling," *IEEE Trans. Control Syst. Technol.*, vol. 10, no. 1, pp. 43–54, Jan. 2002.
- [14] J. Marzbanrad, G. Ahmadi, H. Zohoor, and Y. Hojjat, "Stochastic optimal preview control of a vehicle suspension," *J. Sound Vib.*, vol. 275, no. 3–5, pp. 973–990, Aug. 2004.
- [15] K. Yao, D. Chen, W. Huang, and J. Chiang, "Digital control design of decentralized stochastic singularly-perturbed large-scale actuator type systems with multiple time-varying delays," *Int. J. Innovative Comput., Inf. Control*, vol. 5, no. 10(B), pp. 3303–3312, Oct. 2009.
- [16] N. Yagiz, Y. Hacioglu, and Y. Taskin, "Fuzzy sliding-mode control of active suspensions," *IEEE Trans. Ind. Electron.*, vol. 55, no. 11, pp. 3883–3890, Nov. 2008.
- [17] P. Els, N. Theron, P. Uys, and M. Thoreson, "The ride comfort vs. handling compromise for off-road vehicles," *J. Terramechanics*, vol. 44, no. 4, pp. 303–317, Oct. 2007.
- [18] R. Amirifar and N. Sadati, "Low-order H_∞ controller design for an active suspension system via LMIs," *IEEE Trans. Ind. Electron.*, vol. 53, no. 2, pp. 554–560, Apr. 2006.
- [19] S. Türkay and H. Akcay, "Aspects of achievable performance for quarter-car active suspensions," *J. Sound Vib.*, vol. 311, no. 1/2, pp. 440–460, Mar. 2008.
- [20] S. Huang and H. Chen, "Adaptive sliding controller with self-tuning fuzzy compensation for vehicle suspension control," *Mechatronics*, vol. 16, no. 10, pp. 607–622, Dec. 2006.
- [21] S. Tong, T. Wang, and W. Zhang, "Fault tolerant control for uncertain fuzzy systems with actuator failures," *Int. J. Innovative Comput., Inf. Control*, vol. 4, no. 10, pp. 2461–2474, Oct. 2008.
- [22] T. Yoshimura, A. Kume, M. Kurimoto, and J. Hino, "Construction of an active suspension system of a quarter car model using the concept of sliding mode control," *J. Sound Vib.*, vol. 239, no. 2, pp. 187–199, Jan. 2001.
- [23] T. Iwasaki and S. Hara, "Generalized KYP lemma: Unified frequency domain inequalities with design applications," *IEEE Trans. Autom. Control*, vol. 50, no. 1, pp. 41–59, Jan. 2005.
- [24] T. Iwasaki and S. Hara, "Feedback control synthesis of multiple frequency domain specifications via generalized KYP lemma," *Int. J. Robust Non-linear Control*, vol. 17, no. 5/6, pp. 415–434, Mar./Apr. 2007.
- [25] W. Rattasiri and S. Halgamuge, "Computationally advantageous and stable hierarchical fuzzy systems for active suspension," *IEEE Trans. Ind. Electron.*, vol. 50, no. 1, pp. 48–61, Feb. 2003.
- [26] X. Yu and O. Kaynak, "Sliding-mode control with soft computing: A survey," *IEEE Trans. Ind. Electron.*, vol. 56, no. 9, pp. 3275–3285, Sep. 2009.
- [27] Z. Wang, D. Ho, Y. Liu, and X. Liu, "Robust H_∞ control for a class of nonlinear discrete time-delay stochastic systems with missing measurements," *Automatica*, vol. 45, no. 3, pp. 684–691, Mar. 2009.
- [28] Z. Wang, Y. Liu, and X. Liu, " H_∞ filtering for uncertain stochastic time-delay systems with sector-bounded nonlinearities," *Automatica*, vol. 44, no. 5, pp. 1268–1277, May 2008.



Weichao Sun received the B.S. degree in automation from Central South University, Changsha, China, in 2007 and the M.S. degree in control science and engineering from the Harbin Institute of Technology, Harbin, China, in 2009, where he is currently working toward the Ph.D. degree in the Research Institute of Intelligent Control and Systems.



Ye Zhao is currently working toward the B.S. degree in the Research Institute of Intelligent Control and Systems, Harbin Institute of Technology, Harbin, China.



Jinfu Li is currently working toward the B.S. degree in the Research Institute of Intelligent Control and Systems, Harbin Institute of Technology, Harbin, China.



Lixian Zhang received the Ph.D. degree in control science and control engineering from the Harbin Institute of Technology, Harbin, China, in 2006.

He was a Postdoctoral Fellow with the Mechanical Engineering Department, Ecole Polytechnique de Montreal, Montreal, QC, Canada, from December 2006 to October 2008. He joined Harbin Institute of Technology in January 2009, where he is currently an Associate Professor. His research interests include switched systems and their applications, etc.



Huijun Gao (SM'09) received the Ph.D. degree in control science and engineering from the Harbin Institute of Technology, Harbin, China, in 2005.

He was a Research Associate with the Department of Mechanical Engineering, The University of Hong Kong, Hong Kong, Hong Kong, from November 2003 to August 2004. From October 2005 to October 2007, he carried out his postdoctoral research at the Department of Electrical and Computer Engineering, University of Alberta, Edmonton, AB, Canada. Since November 2004, he has been with

the Harbin Institute of Technology, where he is currently a Professor and the Director of the Research Institute of Intelligent Control and Systems. He is an Associate Editor for *Automatica*. His research interests include network-based control, robust control/filter theory, time-delay systems, and their engineering applications.

Dr. Gao is an Associate Editor for *IEEE TRANSACTIONS ON INDUSTRIAL ELECTRONICS*, *IEEE TRANSACTIONS ON SYSTEMS, MAN, AND CYBERNETICS—PART B: CYBERNETICS*, *IEEE TRANSACTIONS ON FUZZY SYSTEMS*, and *IEEE TRANSACTIONS ON CIRCUITS AND SYSTEMS—I*.